ТЕХНОЛОГИИ ОБРАБОТКИ МАТЕРИАЛОВ

UDC 621.73 DOI:10.18503/1995-2732-2016-14-1-69-78

BEHAVIORS OF BULK METALLIC GLASS UNDER SHOCK LOADING

Atroshenko S.A.

Institute for Problems of Mechanical Engineering, Russian Academy of Science, Saint Petersburg, Russia

Abstract. The high-strain-rate method of materials for dynamic strength investigations under micro and submicrosecond durations of shock loads on the base of electrical explosion of conductors have been developed. The experimental investigations of dynamic properties for bulk metallic glass on the base of Ti and Zr under shock loads of submicrosecond duration (~0.5-0.7 μs) in the pressure range up to 12 GPa have been carried out. The values of Hugoniot elastic limit (HEL) and spall strength for these amorphous alloys have been received. The Hugoniot shock adiabat parameters were determined in the space U_{sh} - u_p. The result of microstructure analysis of saved specimens revealed areas of recrystallization.

Keywords: bulk metallic glass, shock load, electrical explosion of conductors, dynamic strength, Hugoniot elastic limit, spall strength.

Introduction

The solution of many technical problems is connected with understanding the processes of the appearance and the propagation of shock waves, with knowledge on physical-mechanical parameters defining behavior of materials under high-strain-rate. The investigation of shock-wave processes in the materials gives possibility to receive information on interconnection for materials microstructure and macroscopic parameters defining their behavior under pulse loading and about the influence on the dynamic strength of solids.

More information on the influence of correlation of material scale level structure and dimensional-temporal spectrum of shock loading on material behavior under high-strain-rate and on threshold and peculiarities of fracture process can be received under improvement and development of experimental techniques for creation of shock loads with different temporal profiles. The reproducibility of techniques for different experiments play important role in these investigations. The application of electrical explosion of conductors is one of perspective directions for realization of such problems [1]. This technique permits up to 40–50% of provided electrical power to transform to kinetic energy of explosive products.

Bulk metallic glasses are very attractive field for investigations because of their unique chemical and physical-mechanical properties last time. Nevertheless the brittleness of the amorphous materials hinders their broad application [2, 3]. The different specimens of the amorphous alloy with the same composition can have essentially different plasticity levels depending on cooling velocity under crystallization, presence of nanocrystalline phase, concentration of the free volume.

The investigation of the bulk metallic glass behavior under high-strain-rate was the aim of this work. It was developed technique using the electrical explosion of conductor phenomenon for the shock load generation in solids [1]. This method permit to extend essentially the changing range of the shock load parameters. The application of the modern interferometric methods for checking of the load parameters and the metallographic investigations of the specimen structure before and after shock loading allow to receive considerable information on the development of deformation processes, structure kinetics and fracture of the materials under high-strain-rate.

Material behaviors under conditions of high strain rates are of practical importance with the rapid development of military and aerospace technology. Bulk metallic glasses (BMGs), as a class of advanced structural and functional materials, which possess a combination of outstanding properties including ultrahigh strength, high hardness, large elastic limit, unique fracture toughness, and excellent corrosion resistance [2–3], have gradually gained considerable attention from materials science community. It should be of scientific and technological interest to probe the deformation behaviors of BMGs under plate impact loading in order to shed lights on the high strain-rate response of this advanced materials and for their great potential applications, such as kinetic energy penetrators.

I. Dynamic behavior of bulk metallic glass on the base of Ti

Authors [4] studied the shock wave response of (Hf,Zr)-based bulk amorphous alloy specimens subjected to peak stresses of 4–16 GPa in plate impact experiments and their response was compared to a previously studied Zr-based BMG and reported that the (Hf,Zr)-based BAA displayed a Hugoniot elastic limit (HEL) of 7.4 GPa corresponding to an elastic strain of 4.3%. Turneaure and his co-workers [5,6] reported that the HEL stress of $Zr_{56.7}Cu_{15.3}Ni_{12.5}Nb_{5.0}Al_{10.0}Y_{0.5}$ BMG was determined to be 7.1 ± 0.3 GPa and 8.97±0.61 GPa in [7]. In [5] a Zr-based BMG subjected to uniaxial tensile strain in plate-impact experiments under compressive loading with peak stresses ranging between 3.9 and 6.1 GPa, in the result of wave interactions produced tensile loading leading to spallation in the BMG samples. Tensile fracture or spall, observed in these experiments, was initiated at a tensile stress of 3.8±0.3 GPa and 3.6±0.1 GPa in [7]; this value was independent of the impact stress and is significantly higher than that observed for crystalline metals. T. Mashimo with co-authors [8] stated the HEL stress of $Zr_{55}Al_{10}Ni_5Cu_{30}$ BMG was 6.2 GPa. The Hugoniot elastic limits were determined to be 6.9 to 9.6 GPa [9]. Yuan *et al.* [10] conducted plate-impact experiments to investigate the shock response of a Zr-based BMG, in the normal stress range of 5–7 GPa. The HEL of the BMG was estimated to be 6.15 GPa. The above experiments are of importance to understand the equations of state (EOS), constitutive equations and damage mechanism of bulk glass-forming alloys upon dynamic loading. However, very limited data are currently available for the dynamic compression properties of Ti-based bulk glassy alloys.

In this paper, shock wave compression experiments were performed on the $Ti_{40}Zr_{25}Ni_3Cu_{12}Be_{20}$ BMG in order to gain better understanding of the response features upon shock loading. Recovery experiment was also carried out in order to investigate the structure of shock-compressed samples.

In the present work, the shock responses of $Ti_{40}Zr_{25}Ni_3Cu_{12}Be_{20}$ bulk metallic glass (BMG) were investigated by using a planar impact technique on an electrical explosion of conductor (EEC) installation. The spallation occurs even if the stress behind the shock front is less than the Hugoniot elastic limit (HEL) stress of the Ti-based BMG. When the velocity of aluminum flyer with thickness of 1.7 mm is 570 m/s, the spall strength of the alloy sample is 2.9 GPa while the stress, strain and particle velocity behind the shock front are 4.3 GPa, 2.8% and 150 m/s, respectively. The calculated yield strength for the alloy upon the dynamic loading is much larger than that under the quasistatic compressive loading. The microscopy observation indicates that, after dynamic loading, the free surface of the sample exhibits formation of a lot of shear bands and cracks. Optical microscope shows that cracks and microvoids, which caused the occurrence of the spallation of the sample, are distributed on the cross-section of the recovered Ti-based BMG sample.

1.1 Experimental

Alloy ingots with the nominal composition $Ti_{40}Zr_{25}Ni_3Cu_{12}Be_{20}$ (at. %) were prepared from a mixture of constituent elements with purities better than 99.9% (wt. %), by non-consumable arc melting under a Ti-gettered argon atmosphere. To ensure composition homogeneity, each ingot was remelted at least four times. Bulk glassy samples were prepared by remelting the button ingots and drop casting the molten alloy into a copper mold with an internal cavity of 3×30×80 mm^3. The structure of the plate-shaped samples were identified by X-ray diffraction (XRD) using the Cu Kα radiation [3].

Before dynamic compression experiments elastic characteristics for the glass were measured. Density, ρ_0, of the sample was measured by an Archimedean method and averaged over several samples cut from different positions of each plate. Longitudinal C_l and transverse C_t wave velocities were determined by testing the acoustic signals oscillograms in glassy samples. Elastic constants of the glass were calculated and listed in Table 1 [3].

Table 1

Density and elastic characteristics for $Ti_{40}Zr_{25}Ni_3Cu_{12}Be_{20}$ bulk metallic glass

ρ_0, g/cm^3	C_l, m/s	C_t, m/s	E, GPa	K, GPa	G, GPa	v
5.44±0.01	5295±10	3180±30	134	79	55	0.218

here K is the bulk modulus, G is the shear modulus, E is the elastic Young's mudulus, and v is the Poisson ratio.

The dynamic strength investigations of the bulk glassy samples were performed by plane plate impact technology on an electrical explosion of conductor installation (EEC). The glass samples were in the form of plate with a size of 3×30×30 mm^3 and the flyers were in the form of a disk, 20 mm in diameter and 1.7 mm in thickness. The parameters of EEC are as follow: capacitance C is 6 μf, voltage U is 50 kV, total energy E is up to 7.5 kJ, short circuit duration T is 11 μs. Velocities of the aluminum impactor range from 250 to 750 m/s, controlled by a differential laser interferometer. Plasma energy generated by explosion of conductors is used for projectile acceleration, allowing the investigations of submicrosecond shock duration within a velocity rate of 1000~1500 m/s. The scheme for spall testing is presented in Fig. 1. The fracture morphology of

the tested samples was examined by microscopy using Axio-Observer Z1 M microscope to reveal the deformation and fracture mechanism.

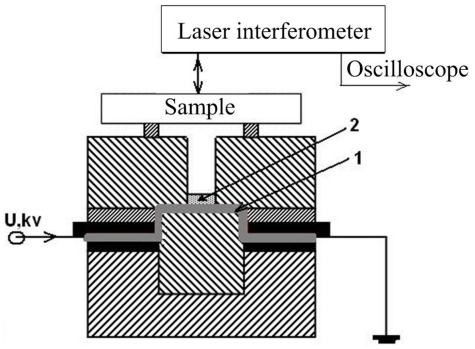

Fig. 1. Schematic illustraion of the set-up for spall strength investigation: 1 – exploding foil (aluminum foil with dimensions 0.01×20×50 mm³); 2 – plate-flyer from aluminum alloy with dimensions ∅20×1.7 mm³ [3]

1.2 Results and Discussion

Fig. 2 shows the XRD pattern of the $Ti_{40}Zr_{25}Ni_3Cu_{12}Be_{20}$ alloy, which consists of only a typical broad diffused peak. No evidence of any Bragg crystalline peaks can be observed from the XRD pattern within the detectable limitation of the XRD, typical of a glassy nature.

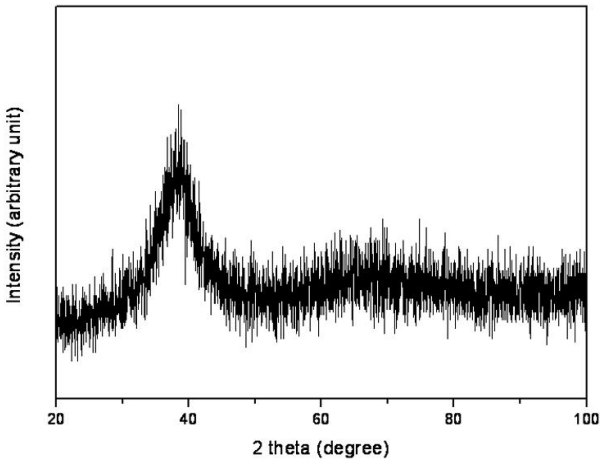

Fig. 2. XRD pattern for the as-cast $Ti_{40}Zr_{25}Ni_3Cu_{12}Be_{20}$ bulk glassy sample [3]

Fig. 3 shows the interferogram and the corresponding velocity profile at the free surface for $Ti_{40}Zr_{25}Ni_3Cu_{12}Be_{20}$ BMG samples impacted by Al flyer at the impact velocity of 570 m/s. As can be seen from Fig. 3, the free surface particle velocity firstly raised to 300 m/s without a kink, suggesting that only elastic shock wave propagated within the sample and the stress behind the shock front was lower than the HEL stress. Then the free surface particle velocity rapidly dropped down to 90 m/s, followed by a small fluctuation, indicating the occurrence of spallation within the sample under dynamic loading.

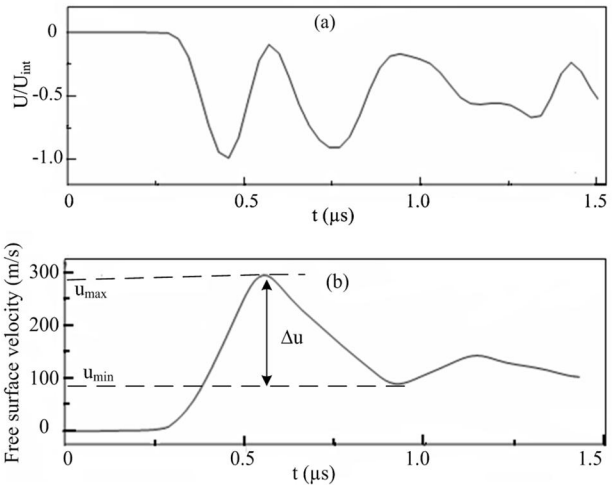

Fig. 3. Interferogram (a) and corresponding free surface velocity profile (b) obtained for $Ti_{40}Zr_{25}Ni_3Cu_{12}Be_{20}$ glassy samples impacted by Al flyer at the impact velocity of 570 m/s [3]

Fig. 4 shows a schematic of wave propagation in the flyer and the target BMG sample (*t*-*X* diagram) for a typical plate-impact spall experiment. The horizontal coordinate represents the distance in the target and the flyer from the impact surface, while the longitudinal coordinate represents the time after impact. As shown in Fig. 4, upon impact, compressive waves are generated in both the target and the flyer plates. After reflected from the free surface of the flyer or target BMG, compressive waves would change into the rarefaction waves and propagate to an opposite direction. When the rarefaction waves reflected from the free surfaces of the flyer and the sample interacts at a predetermined location, A, within the BMG sample, the sample begins to subject to tensile stress. As we know for a material when the tensile stress reaches a level beyond its ability to resist fracture, it fails in a process known as spallation (Region 7). The material's spall strength can be calculated by the following equation:

$$\sigma_{spall} = \frac{1}{2}\rho_0 C_l \Delta u \qquad (1)$$

where Δu can be calculated by the difference between the free surface particle velocity $u_{\max}$ and $u_{\min}$, which can be obtained from free surface velocity profile shown in Fig. 3b. According to Eq. (1), the corresponding value of spall strength for $Ti_{40}Zr_{25}Ni_3Cu_{12}Be_{20}$ glassy samples can be estimated to be 2.9 GPa.

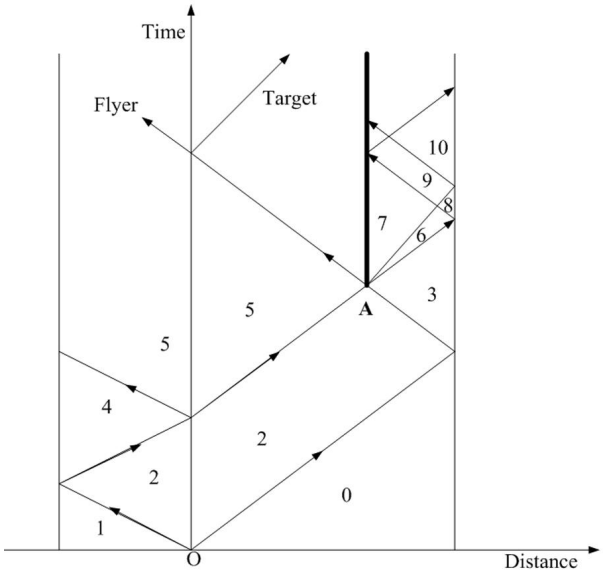

Fig. 4. Wave propagation in the flyer and the target BMG sample (*X-t* diagram) for a typical plate-impact spall experiment. The arrows indicate the direction of wave propagation [3]

When the stress behind the shock front is less than the HEL stress of the material, the shock wave velocity could be replaced with the longitudinal wave velocity of the material. The stress and the strain behind the shock front can be evaluated by the below relations:

$$\sigma_x = \rho_0 C_l u \tag{2}$$

$$\varepsilon = \frac{u}{C_l} \tag{3}$$

where u is the particle velocity behind the shock front which is equal to half of the maximum free surface particle velocity. The corresponding values for σ_x and ε are 4.2 GPa and 2.7 %, respectively.

Using the von Mises yield criterion, the yield strength, Y_0, under uniaxial stress loading can be readily computed by the following expression:

$$Y_0 = \frac{1-2\nu}{1-\nu}\sigma_{HEL} \tag{4}$$

Considering that σ_x is below the HEL stress of the material in this study, replacement of σ_{HEL} with σ_x into equation (4) gives:

$$Y_0 > \frac{1-2\nu}{1-\nu}\sigma_x \tag{5}$$

Using the ambient value of ν, accordingly, Y_0 of the glassy alloy studied is larger than 3.0 GPa. For comparison, the quasistatic compression tests on the Ti-based alloy with the same composition gives Y_0 = 1.8 GPa [11]. Such discrepancies in the yield strength obtained from different types of loading have been previously observed in Zr-based glass, for which the yield strength obtained from plate impact experiments (uniaxial strain) and quasistatic compression experiment (uniaxial stress) are 2.83 and 1.9 GPa, respectively [12, 13]. HEL and yield stress in a ternary BMG, $Zr_{50}Cu_{40}Al_{10}$ are determined as 6.8 GPa and 2.8 GPa, respectively [14].

After the dynamic loading experiment, the soft-recovered samples were observed under mycroscopy. Fig. 5 shows the typical micrograph for free surface of the shocked sample. Many cracks and shear bands can be observed on the free surface of the shocked sample. The similar phenomenon - multiple parallel shear bands oriented at 45° to the loading direction were observed on the surfaces of the deformed specimens $Zr_{41.5}Ti_{13.5}Cu_{12.5}Ni_{10}Be_{22.5}$ BMG [15]. The formation of the shear bands and cracks on the free surface of the shocked sample is caused by to the shear localization within the sample during the shock loading.

To characterize the damage area around the spall plane of the $Ti_{40}Zr_{25}Ni_3Cu_{12}Be_{20}$ BMG, the cross-section of the shocked samples were observed. Fig. 6 shows the typical cross-section optical microscope image of the recovered Ti-based BMG sample. Cracks, which lead to the occurrence of the spallation, can be clearly seen in the damage area around the spall zone. Careful examination reveals that the cracks are formed due to the coalescence of microvoids, as it is seen in Fig. 6 similar data presented in [16], where fracture occurs mostly through the growth and coalescence of damage cavities. Therefore, the spall plane was formed due to the growth and coalescence of those microvoids.

Based on the free volume theory and Spaepen's model [17–18], one can conclude that the free-volume concentration is strongly sensitive to the strain rate, i.e. increasing strain rate could result in an significant increase in the free-volume concentration. Under the shock wave loading, a large number of free volumes would be created in the amorphous alloy due to extremely high strain rate (higher than 10^4 s^{-1}). The free volumes in the pre-determined location, A, as marked in Fig. 4, where the rarefaction waves interacts, would spontaneously coalescence to microvoids due to the tensile stress. The local increase in microvoids has been suggested as the main mechanism for nucleation of cracks. Once the cracks nucleate, they will propagate rapidly, therefore, causing the spallation of the sample. Thus, lots of microvoids and cracks could be seen in the damage area around the spall plane of the sample.

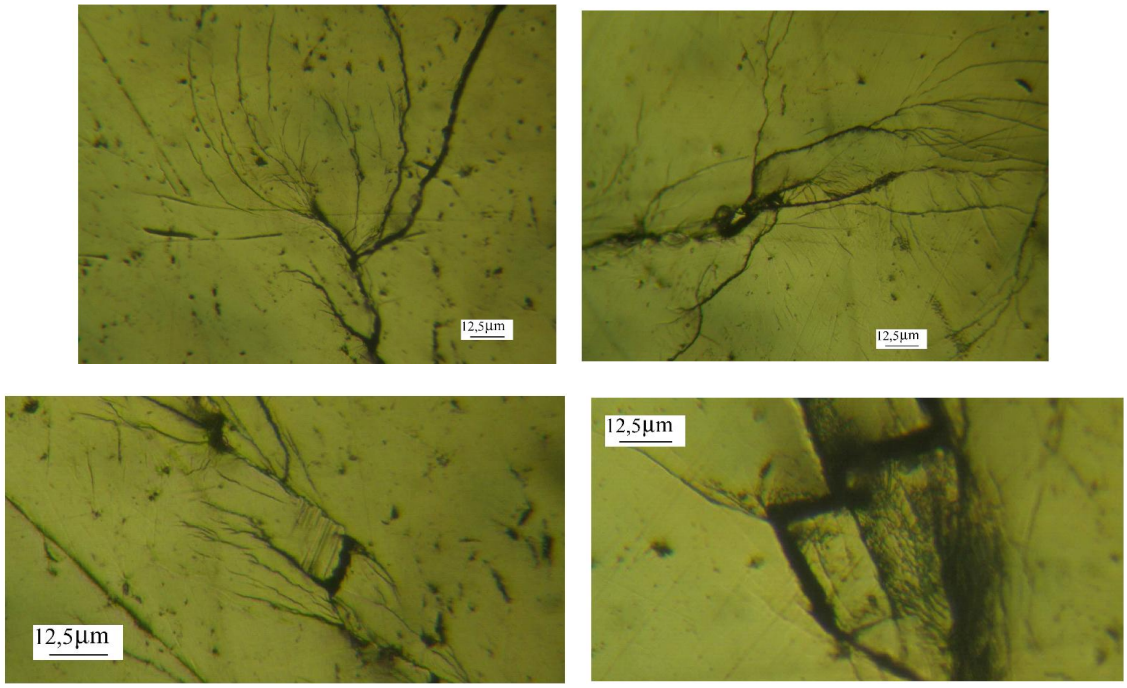

Fig. 5. Typical free-surface micrograph of the recovered Ti40Zr25Ni3Cu12Be20 BMG sample after shock loading

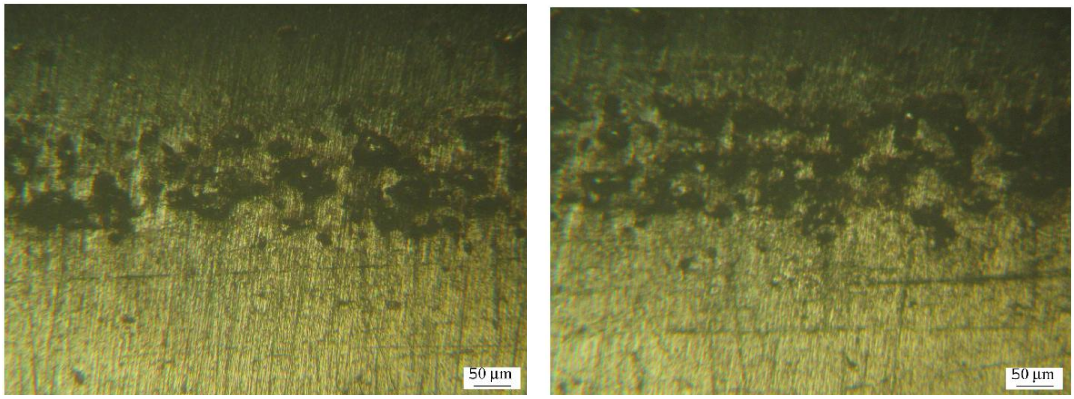

Fig. 6. Typical cross-section optical micrograph of the recovered $Ti_{40}Zr_{25}Ni_3Cu_{12}Be_{20}$ BMG sample showing the damage area around the spall zone

1.3. Conclusions

From the results discussed above, several conclusions can be drawn as follows:

(1) Spallation of the Ti-based bulk metallic glass in dynamic loading occurs prior to yielding.

(2) The yield strength of the Ti-based metallic glass under the dynamic loading is larger than the reported quasistatic value.

(3) Cracks and microvoids, which caused the occurrence of the spallation of the sample, are distributed on the cross-section of the recovered Ti-based BMG sample.

II. Dynamic behavior of bulk metallic glass on the base of Zr

The purpose of this study is to experimentally investigate the deformation and microstructural changes of Zr-based bulk metallic glass (BMG) under high-strain-rate.

2.1. Experimental procedure

The investigation of the dynamic properties for metallic glass was carried out using the electrical explosion of conductors installation with following parameters: capacitor C = 6 μf, voltage U up to 50 kV, stored energy $E \leq 7.5$ kJ, short-circuit duration T = 10.5 μs [2].

The technique for the creation of shock load was developed: direct or via plate-waveguide loading of the specimens by shock wave under foil explosion. The temporal dependence of the specimen free surface velocity at the outlet of the pressure pulse on the surface has been checked with the help of the differential laser interferometer (delay time τ = 0.4 ns) [19, 20].

Fig. 7 shows the chart of the technique using symmetry of the foil explosion which permits to receive the information about shock load parameters both at the front and in the back specimen surface with good accuracy.

Specimens were in the form of plates with dimensions ø30×3 mm. Specimens were prepared by arc melting and continuous casting.

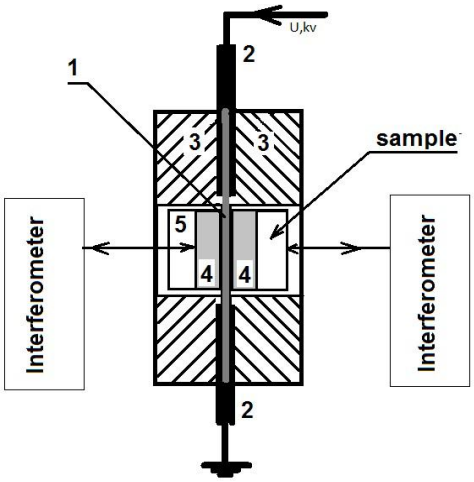

Fig. 7. Shock wave loading by foil explosion:
1 – aluminum foil 0.03×20×35 mm, 2 – electrodes,
3 – the frame from dielectric, 4 – waveguide
(ceramic, polymer), 5 – optical window (PMMA,
quartz glass, sapphire) [2]

The movement velocities of free surfaces for waveguide and specimens were monitored using differential interferometers. Exploding aluminum foil was placed between two ceramic waveguides ø35 mm in diameter and equal thickness, the optical glass and specimen were in acoustic contact with these waveguides on different sides from them. This technique permitted to define with good accuracy both the moment of the specimen loading and the starting load parameters. At the same time this technique could determine the load transformation under pulse passing across the specimen.

2.2 Results and Discussion

Experimental investigations of the behavior of the amorphous metallic glass on the base of Zr under shock loads of 0.5 μs duration in the pressure range ≤12 GPa could be carried out due to developed techniques.

Preliminary velocities of elastic waves were measured in metallic glasses specimens with the help of optical-acoustic technique [21] and elastic modulus was calculated (Table 2). For comparison, this table also shows the data for the metallic glass on the base on titanium.

Table 2

The results of measurements and calculations

Amorphous alloys	ρ, g/cm³	C, m/s	C_t, m/s	E, GPa	G, GPa	ν
$Ti_{40}Zr_{25}Ni_3Cu_{12}Be_{20}$	5.44±0.01	5295 ±10	3180±30	134± 3	55 ±1.5	0.218
ZrNiCuAl	6.810±0.005	4900±10	2360±20	102± 2	38±1.0	0,349

Temporal profiles of the free surface velocity under different loading intensities are presented in Fig. 8.

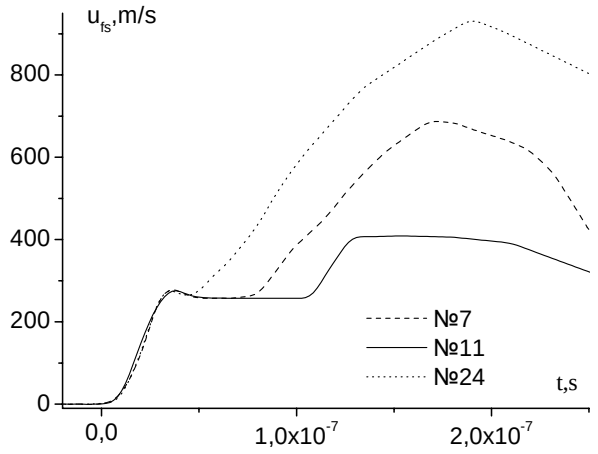

Fig. 8. Temporal profiles of the free surface velocity for specimens from ZrNiCuAl alloy under different intensity of the loading. The dotted line shows the profile of mass velocity of particles at the boundary of the ceramic waveguide and the optical window

It is clearly seen two-wave structure of the wave typical for elastic-plastic response of the materials. Still further this structure is specific for almost ideally plastic response. It follows from the presence of practically horizontal part of the profile after loading front. It is seen the specific tooth of flow. Dynamic elastic limit determined in the experiments is equal σ_{HEL}=4.57±0.05 GPa and spall strength for ZrNiCuAl alloy is equal σ_{sp}=4.43±0.05 GPa. The spall strength was calculated by the method based on the difference between the peak velocity and the first minimum in the free surface velocity profiles and the product of the initial density and longitudinal wave speed [20].

The parameters of the shock Hugoniot adiabat in the space of velocity of the shock wave U_{sh} and the particle velocity u_p are presented in Fig. 9.

Several Us-Up curves of Zr based BMGs reported in literatures [7]. It can be seen that a kink appears at particle velocity 380m/s ~ 660m/s (pressure range 14GPa ~ 26GPa) for Zr-based BMGs, and for $Zr_{57}Nb_5Cu_{15.4}Ni_{12.6}Al_{10}$ BMG, a second kink appears at 1.7km/s. In present experiments a kink appears at lower particle velocity ~180m/s.

Microstructural examination of samples after high-strain-rate showed that the free surface cracks have an oval semi-closed form, forming a chain (Fig. 10a). Also, on the free surface of the sample multiple deformation bands placed parallel each other are seen (Fig. 10b – in polarized light). Shear bands are typical for the microstructure of the shock loaded Zr based BMG material.

In the test modes, the material is characterized by the appearance of specific areas of localization of deformation in the form of increased etched regions as it shown in Fig.10 (c, d).

The cross-section shows typical spall split (Fig. 11a), perpendicular to the wave propagation direction or spall zigzag split (Fig. 11b), placed at an angle of 450 to the direction of wave propagation.

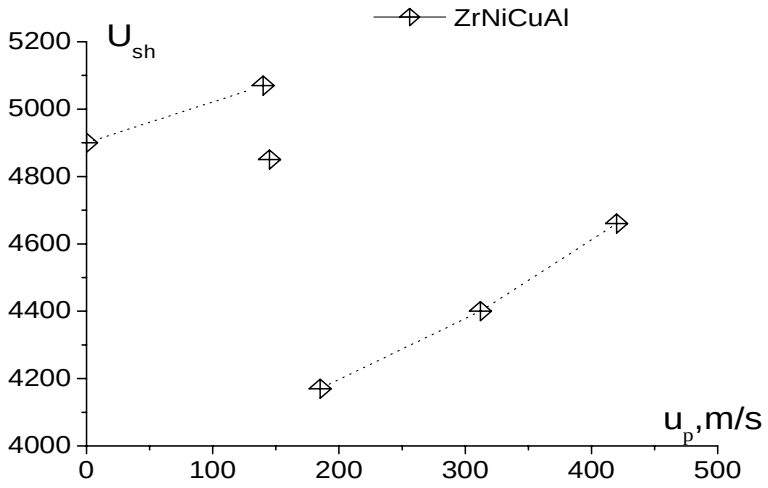

Fig. 9. Dependence $U_{sh} = f(u_p)$ for ZrNiCuAl alloy

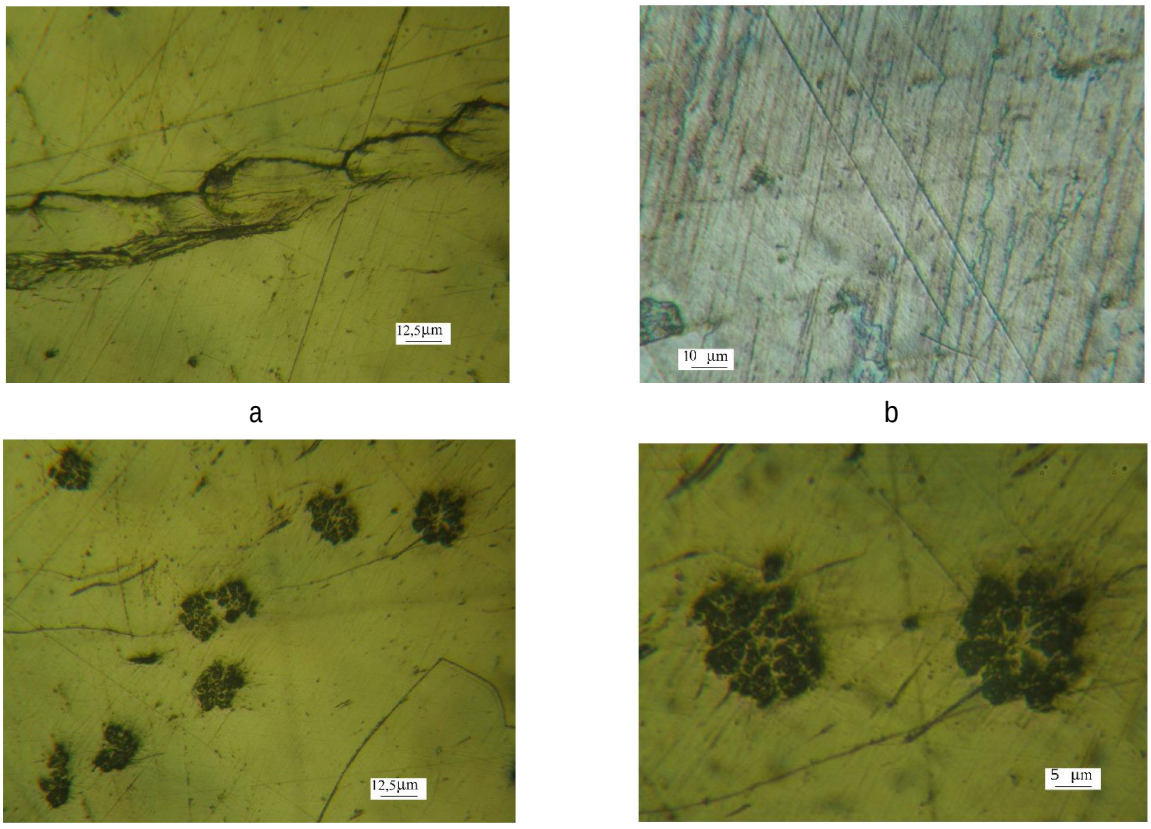

a b

c d

Fig. 10. Free surface of ZrNiCuAl shock loaded specimens

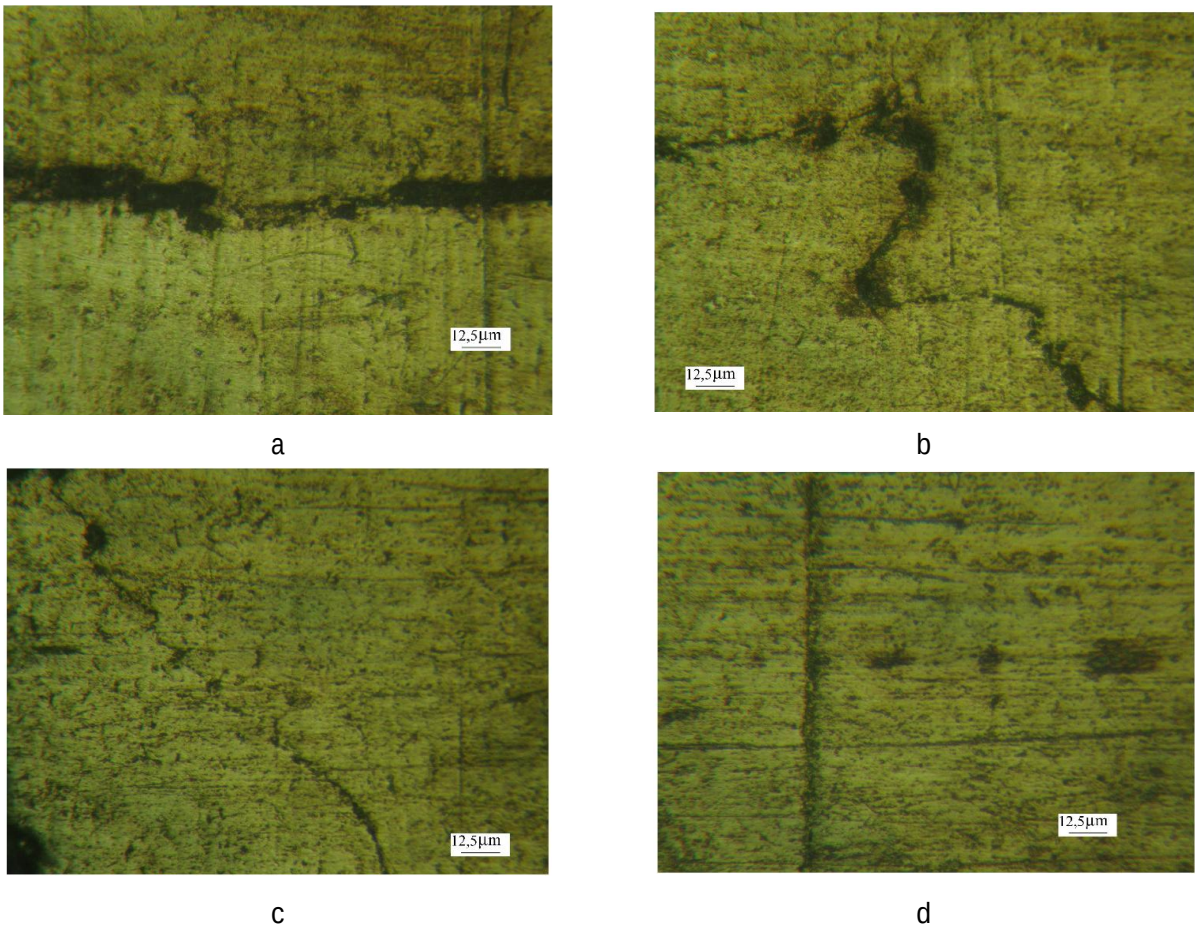

Fig. 11. Microstructure of the cross-section for ZrNiCuAl BMG shock loaded specimens

The shear bands are arranged in the wave propagation direction (Fig. 11d), and at a certain angle (close to 45°).

Microstructural studies of the samples showed the presence of non-etched areas with fine-grained structure. In these areas under shock loading the conditions necessary for the occurrence of dynamic recrystallization are created. Near free surface of the specimen, i.e. in the region of high strain rate, it is seen in polarized light the areas of dynamic recrystallization (white in Fig. 12) consisting on nanocrystals [22]. Figure 12a presents the cluster of recrystallization areas near the free surface. Typically, recrystallization region in the samples of the material have a shape close to a circle (Fig. 12b). At the same figure it is seen shear bands along the wave propagation direction (Fig. 12a).

The presence of localized shear bands and areas of recrystallization can be conditioned by the sufficiently great amount of free volume (i.e., structural defects), which is formed in the manufacture of the specimens [17, 18]. The localization of defects leads to the formation of zones with the different material parameters and hence to the nucleation of shear bands and to the transformation of the grains.

Mescheryakov and Atroshenko et al. [22, 23] have shown that in the field of shear localization can be quite large absolute values of shear strain and significant, although insufficient to melt, rise of temperature. So in the fields of the shear localization can be expected the processes with formation of the new crystal structure.

XRD analysis of samples №11 and №17 showed (Fig. 13, Table 3) that the appearance of the crystallized structure is observed: a sample №11 – 4,6% of crystals, in a sample №17 – 0.7%. At the same time the increasing of the percentage of crystallinity leads to decreasing of the average size of the zones of recrystallization (the average size of the regions of recrystallization for sample number 11 is 9.7 microns, and for the sample №17 is 16,0 microns). Also, one can see an increase in the values of microhardness for sample №11 HV = 3758 MPa and sample №17 – HV = 3438 MPa.

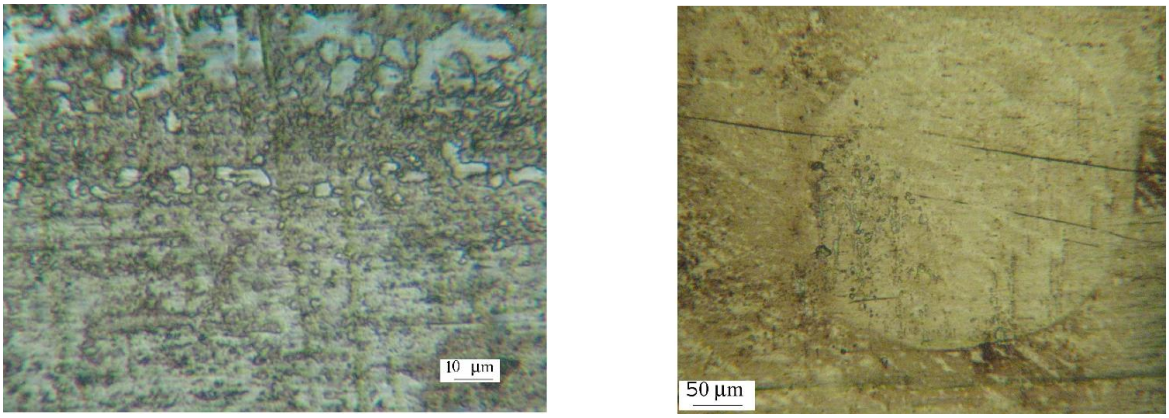

a b

Fig. 12. Dynamic recrystallization in cross-section of the ZrNiCuAl specimens after shock loading: a) nucleus; b) “pancake” pocket of the nanocrystallization

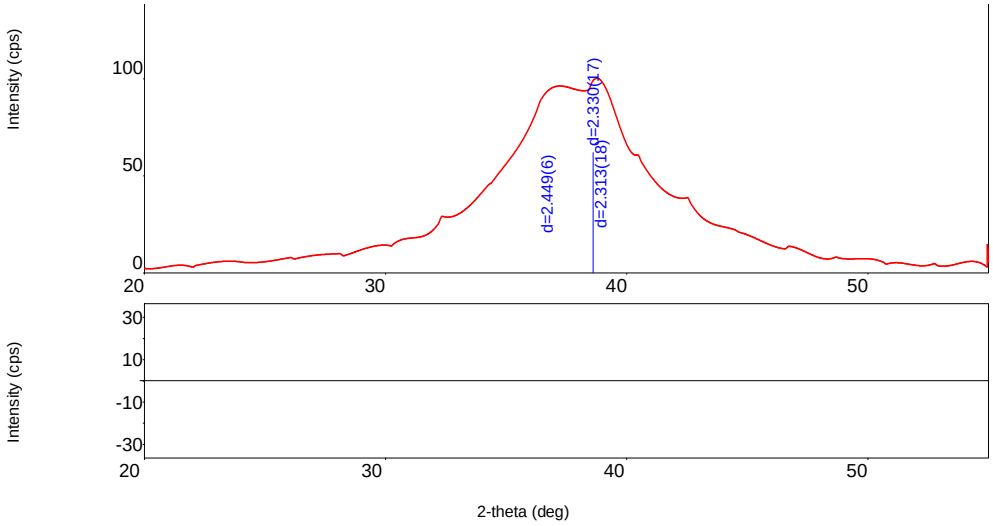

Fig. 13. X-ray measurement profile for specimen №11

Table 3

Dependence of crystallinity quantity in shock loaded specimens on microhardness and dynamic recrystallization areas

Sample №	% of the crystallinity	HV, MPa	Size of areas of dynamic recrystallization, μm		
			Average	Minimum	Maximum
11	4,6%	3758	9,4	2,9	79,6
17	0,7%	3438	16,0	3,7	49,4

2.3. Conclusions

From the above results one can draw the following conclusions:

The investigations of amorphous metallic alloys on the base of Zr justified the qualitative picture for response of these materials on shock loading.

It was found that for our alloy composition on the base of Zr the HEL value σ_{HEL} and spall strength σ_{sp} are 4.57 and 4.43 GPa correspondingly. Nevertheless, despite the value of the spall strength of less than HEL on the fracture surface are observed local regions with shear bands and grains of recrystallization.

The experimental results indicate a complex deformation process during shock compression.

Acknowledgements

Work was financially supported by RFBR projects № 16-01-00638, 16-51-53006 NSFC and by St. Petersburg State University (Project no. 6.39.319.2014).

References

1. Berezin, G.V., Sudenkov, Yu.V. Investigation of shock waves from the electrical explosion of conductors on the dynamic response of solid barriers, Physical mechanics, 4, 119, 1980 (in Russian).
2. I. Smirnov, Atroshenko S., Yu. Sudenkov, N. Morozov, Wei Zheng, N. Naumova, Jun Shen. Dynamic properties of bulk metallic glass on the base of Zr. Shock Compression of Condensed Matter – 2011, Proceedings of the Conference of the

American Physical Society Topical Group on Shock Compression of Condensed Matter held in Chicago, Illinois, USA June 26 – July 1, 2011. American Institute of Physics Melville, New York, 2012, pp. 1121–1124
3. S.A. Atroshenko, N.F. Morozov, W. Zheng, Y.J. Huang, Yu.V. Sudenkov, N.S. Naumova , Jun Shen. Deformation behaviors of a TiZrNiCuBe bulk metallic glass under shock loading. Journal of Alloys and Compounds 505 (2010) 501–504
4. Jaglinski, T.; Turneaure, Stefan J.; Gupta, Y. M., Effect of compositional variation on the shock wave response of bulk amorphous alloys. Journal of Applied Physics, Volume 112, Issue 6, pp. 063529-063529-8 (2012)
5. S.J. Turneaure, S.K. Dwivedi and Y.M. Gupta. Shock-wave induced tension and spall in a zirconium-based bulk amorphous alloy. J. Appl. Phys. 101, 043514 (2007)
6. S.J. Turneaure, J.M. Winey, Y.M. Gupta. Response of a Zr-based bulk amorphous alloy to shock wave compression. J. Appl. Phys. 100 (2006) 063522
7. Binqiang Luo, Guiji Wang, Fuli Tan, Jianheng Zhao, Cangli Liu, and Chengwei Sun. Dynamic behaviors of a Zr-based bulk metallic glass under ramp wave and shock wave loading. AIP ADVANCES 5, 067161 (2015)
8. T. Mashimo, H. Togo, Y. Zhang, Y. Uemura, T. Kinoshita, M. Kodama, Y. Kawamura. Hugoniot-compression curve of Zr-based bulk metallic glass. Appl. Phys. Lett. 89 (2006) 241904
9. Feng Xi, Yuying Yu, Chengda Dai, Yi Zhang and Lingcang Cai. Shock compression response of a Zr-based bulk metallic glass up to 110 GPa. J. Appl. Phys. 108, 083537 (2010)
10. F.P. Yuan, V. Prakash, J.J. Lewandowski. Spall Strength of a Zirconium-based Bulk Metallic Glass. Proceedings of the XIth International Congress and Exposition June 2–5, 2008 Orlando, Florida USA. 2008. Society for Experimental Mechanics Inc.
11. Huang, Y. J., Shen, J. and Sun, J. F. Bulk metallic glasses: smaller is softer, Applied Physics Letters, vol. 90, 081919, 2007
12. S. J. Turneaure, J. M. Winey and Y. M. Gupta. Compressive shock wave response of a Zr-based bulk amorphous alloy. Appl. Phys. Lett. 84, 1692 (2004)
13. Z.F. Zhang, F.F. Wu, G. He, J. Eckert. Mechanical properties, damage and fracture mechanisms of bulk metallic glass materials. J. Mater. Sci. Technol. 23 (2007) 747
14. L. Lu, C. Li, W.H. Wang, M.H. Zhu, X.L. Gong, S.N. Luo. Ductile fracture of bulk metallic glass Zr50Cu40Al10 under high strain-rate loading. Materials Science & Engineering A 651 (2016) 848–853
15. J. Lu and G. Ravichandran. Pressure-dependent flow behavior of $Zr_{41.2}Ti_{13.8}Cu_{12.5}Ni_{10}Be_{22.5}$ bulk metallic glass, Journal of Materials Research, 18, 2039-2049 (2003)
16. E. Bouchaud, D. Boivin, J. L. Pouchou, D. Bonamy, B. Poon and G. Ravichandran, Fracture through cavitation in a metallic glass, Europhysics Letters, 83, (2008)
17. Frans Spaepen, David Turnbull The activation volume of the diffusivity in amorphous metals. Scripta Metallurgica et Materialia Volume 25, Issue 7, July 1991, Pages 1563–1565
18. F. Spaepen, A microscopic mechanism for steady state inhomogeneous flow in metallic glasses. Acta Metall. 25 (1977) 407. Volume 25, Issue 4, April 1977, Pages 407–415
19. Barker, L.M., and Holenbach, R.E., "Interferometer technique for measuring the dynamic mechanical properties of materials", Review of Scientific Instruments, 36, 1617, 1965.
20. Zlatin, N. A., Mochalov, S. M., Pugachev, G. S., and Bragov, A. M., "Time dependence of the process of metal failure under intensive loads", Fiz. Tverd. Tela, 16(6), 1753, 1974 [in Russian].
21. Sud'enkov, Yu.V., and Sazhko, Z.A., "Acoustooptic Spectroscopy of Metal Structure Modifications under Plastic Deformation Due to Submicrosecond Impulsive Shock Loading", Technical Physics, Vol. 48, N1, 125, 2003
22. Atroshenko, S.A., "Shock-Induced Dynamic Recystallization in Metals", in Recrystallization and Grain Growth (eds. Gottstein, G. and Molodov, D.A., Springer-Verlag), 2001.
23. Mescheryakov, Yu.I., and Atroshenko, S.A., "Dynamic recrystallization in shear bands", in Metallurgical and Materials Applications of Shock-Wave and High-Strain-Rate Phenomena (Eds. L.E. Murr et al Elsevier Science, Amsterdam), 1995, 443–450.

Материал поступил в редакцию 26.01.16.

ИНФОРМАЦИЯ О СТАТЬЕ НА РУССКОМ ЯЗЫКЕ

DOI:10.18503/1995-2732-2016-14-1-69-78

ХАРАКТЕРИСТИКИ ОБЪЕМНОГО МЕТАЛЛИЧЕСКОГО СТЕКЛА ПРИ УДАРНОМ НАГРУЖЕНИИ

Атрошенко С.А.

Институт проблем машиноведения РАН, Санкт-Петербург, Россия

Аннотация. На основе электрического взрыва проводников разработан метод высокоскоростной деформации материалов для исследований динамической прочности при ударных нагрузках микросекундной и субмикросекундной длительности. Проведены экспериментальные исследования динамических характеристик объемного металлического стекла на основе титана и циркония при ударных нагрузках субмикросекундной длительности (~0.5–0.7 мкс) в диапазоне давления до 12 ГПа. Для этих аморфных сплавов получены значения предела упругости Гюгонио и предела прочности на растрескивание. Определены параметры ударной адиабаты Гюгонио в пространстве $U_{sh} - u_p$. В результате анализа микроструктуры сохраненных образцов выявлены области рекристаллизации.

Ключевые слова: объемное металлическое стекло, ударное нагружение, электрический взрыв проводников, динамическая прочность, предел упругости Гюгонио, предел прочности на растрескивание.

Atroshenko S.A. Behaviors of bulk metallic glass under shock loading // Вестник Магнитогорского государственного технического университета им. Г.И. Носова. 2016. Т. 14. №1. С. 69–78. doi:10.18503/1995-2732-2016-14-1-69-78

Atroshenko S.A. Behaviors of bulk metallic glass under shock loading. *Vestnik Magnitogorskogo Gosudarstvennogo Tekhnicheskogo Universiteta im. G.I. Nosova* [Vestnik of Nosov Magnitogorsk State Technical University]. 2016, vol. 14, no. 1, pp. 69–78. doi:10.18503/1995-2732-2016-14-1-69-78